Ordered Hierarchically Micro- and Mesoporous Fe−N_x-Embedded Graphitic Architectures as Efficient Electrocatalysts for Oxygen Reduction Reaction

Aiguo Kong, Xiaofang Zhu, Zhen Han, Youyi Yu, Yongbo Zhang, Bin Dong and Yongkui Shan*

Department of Chemistry, East China Normal University, 500 Dongchuan Road, Shanghai 200241, P. R. China

*Corresponding author. E-mail:ykshan@chem.ecnu.edu.cn

Supporting Information

Experimental section

Synthesis of SBA-15:

Mesoporous SBA-15 silica was prepared using Pluronic P123 and tetraethylorthosilicate (TEOS) according to the reported method. In a typical preparation, TEOS (8.3 g) was mixed with P123 (4.0 g) in HCl solution (1.6 M,160 ml) and stirred at 40 ℃ for 24 h. The mixtures were heated at 150 ℃ for 24 h under static condition in a Teflon-lined autoclave. Resulting white precipitate was filtered, dried at 100 ℃. After it was further calcined at 550 ℃ in air for 4 h, with heating rate of 1 ℃ min^{-1}, mesoporous SBA-15 silica was obtained.

Figure S1 Calibration curves to reversible hydrogen electrode

The crossing potential at zero current was taken to be the potential for the reaction of H^+/H_2 reaction in a H_2-saturated electrolyte using the platinum wires as the working electrode and the counter electrode. Using these crossing potential in different electrolytes, all the reported potentials were calibrated to the reversible hydrogen electrode (RHE) potentials according to the reported method.

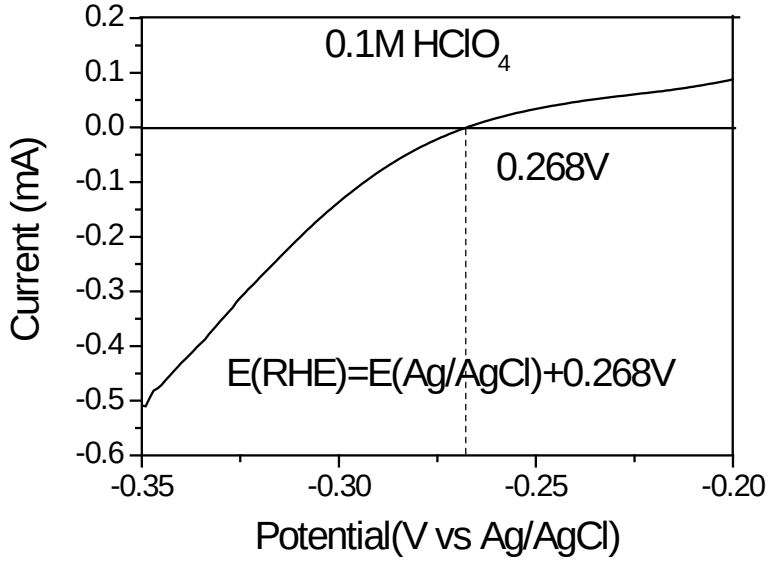

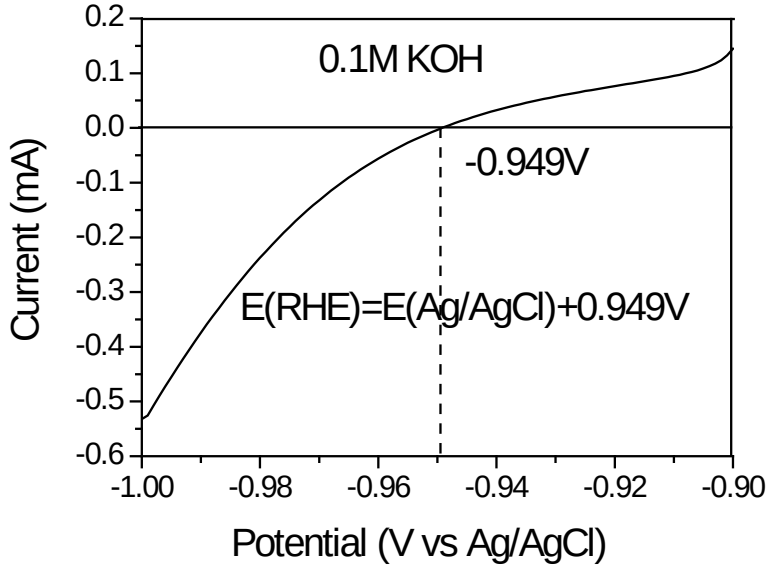

Figure S2 SAED patterns for Fe-N-GC-900

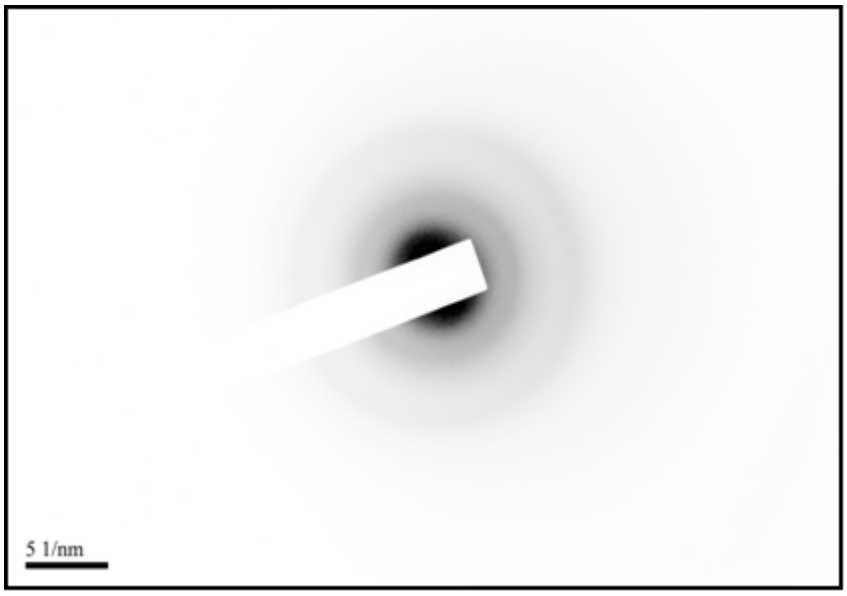

Figure S3 SEM image (A), EDS-mapping images for C (B), Cl (C) and O (D) elements, and the SEM EDS spectrum (E) for Fe-N-GC-900

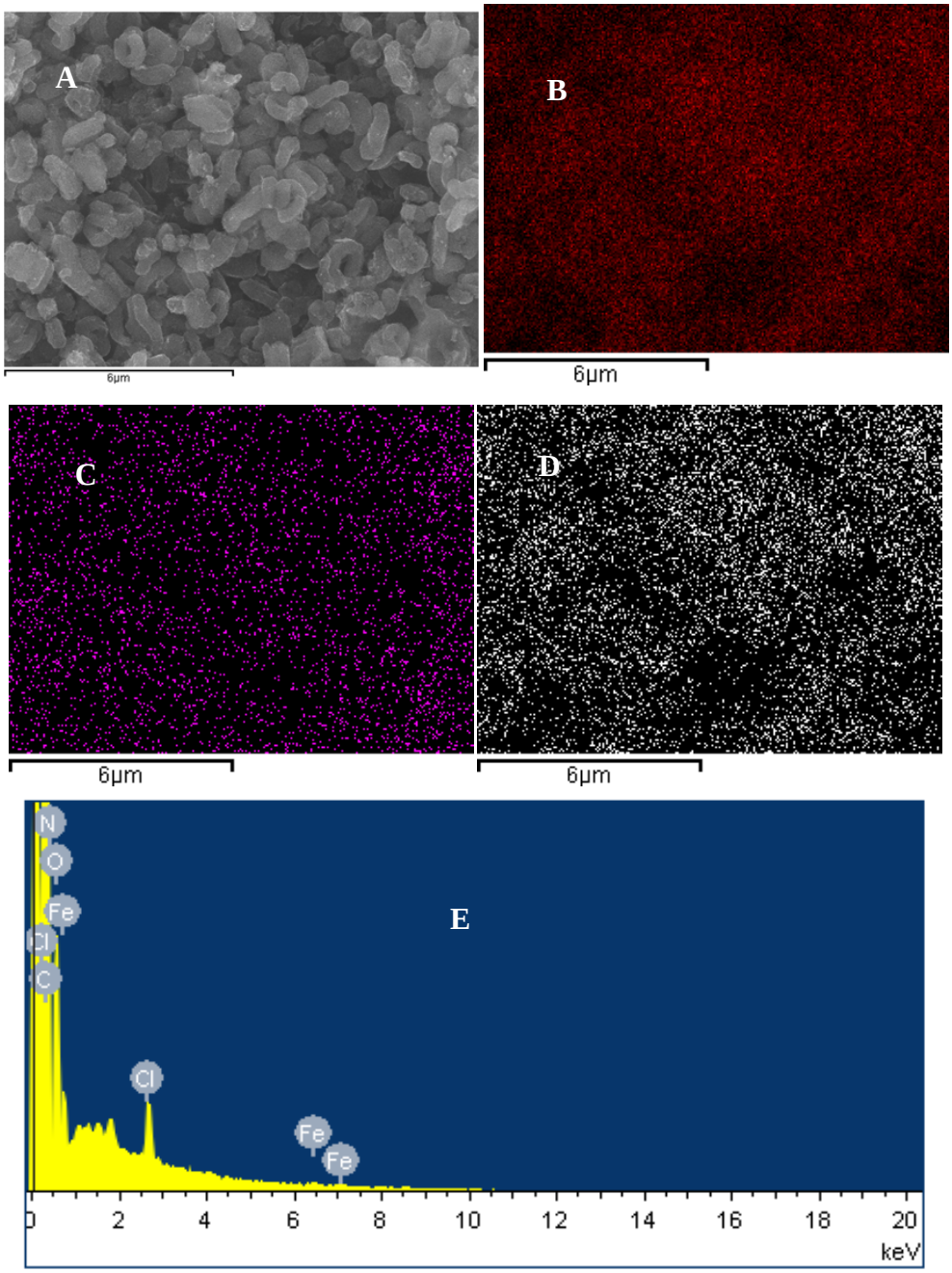

Figure S4 RDE polarization curves at 1600 rpm over Fe-N-GC-900 materials preapred by heating the mixtures containing different molar ratio of 2,2-bipyridine to $FeCl_3$•$6H_2O$ at a scan rate of 10 mV s^{-1} in 0.1 M KOH (A) and 0.1 M $HClO_4$ solution (B)

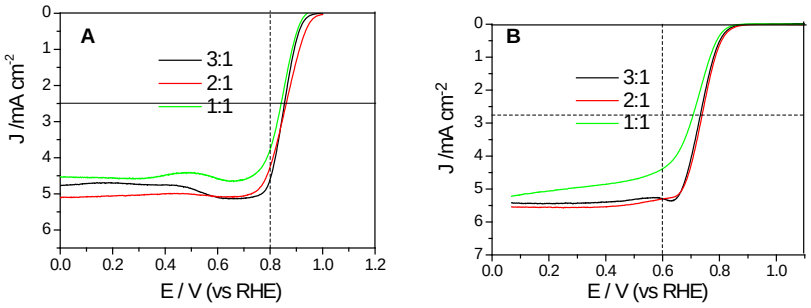

Figure S5 The small-angle (A) and large-angle (B) XRD patterns of Fe-N-GC materials prepared by heating 2,2-bipyridine and $FeCl_3$•$6H_2O$ at different temperatures

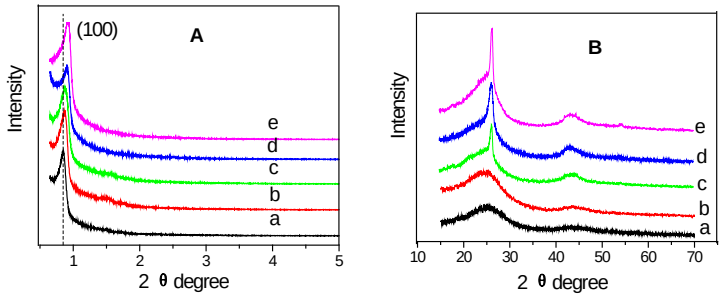

Figure S6 RDE curves recorded at 1600 rpm for Fe-N-GC-900 with different catalyst loadings in an O_2-saturated 0.1 M $HClO_4$ solution at a scan rate of 10 mV s^{-1}

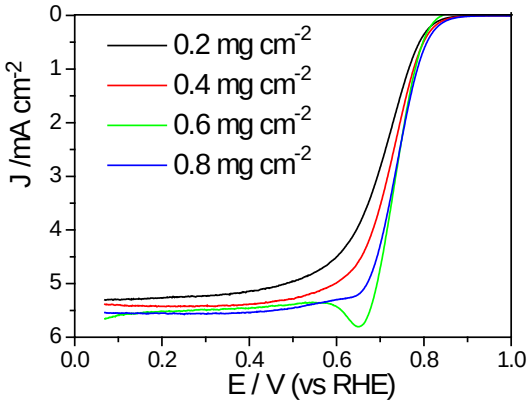

Figure S7 RDE polarization curves for Pt/C-JM recorded at different rotation rates in an O_2-saturated 0.1 M KOH (A) and 0.1 M $HClO_4$ (B) solution and their K-L plots of J^{-1} versus ω^{-1} (C and D)at a scan rate of 10 mV s^{-1}

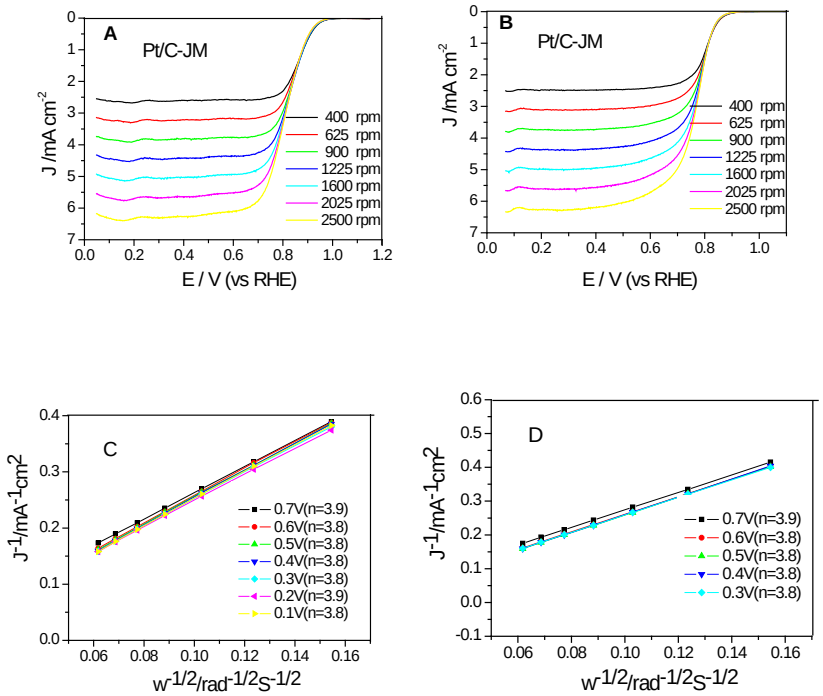

Figure S8 The CV curves on Pt/C-JM electrode with 20ug_{Pt} cm^{-2} loading in a solution of 0.1 M KOH (A) and 0.1 M $HClO_4$ (B) at a scan rate of 10 mV s^{-1}

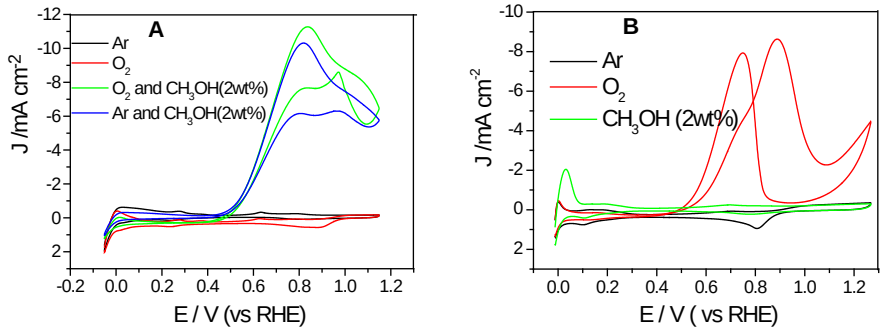

TABLES

Table S1 Textural data of hierarchically porous Fe-N-GC materials

Samples	S_{BET} (cm^2/g)	P_{meso} (nm)	V_{total} (cm^3/g)	$S_{micro}^{T\text{-}plot}$ (cm^3/g)	$V_{Micro}^{T\text{-}plot}$
Fe-N-GC-700-p-aminotoluene	1156	5.0,8.3,12.0	1.90	246	0.12
Fe-N-GC-700-p-nitroaniline	900	4.8	1.05	217	0.10
Fe-N-GC-700-2-amino pyridine	946	5.6	1.19	375	0.19
Fe-N-GC-600	755	5.2	0.98	93	0.04
Fe-N-GC-700	758	5.8	1.16	99	0.05
Fe-N-GC-800	881	6.2	1.28	215	0.105
Fe-N-GC-900	929	6.3	1.35	430	0.21
Fe-N-GC-1000	764	6.5	1.24	145	0.07

Table S2 XPS data for the surface species of Fe-N-GC materials obtained at the different temperatures and their content of deconvoluted N-types

Samples	N (at%)	Metal (at%)	Cl (at%)	Py-N-O (%)	Py-N (%)	G-like (%)	Pyr-N (%)
Fe-N-GC-600	11.3	0.13	0.30	8.27	51.91	12.37	27.45
Fe-N-GC-700	8.66	0.13	0.34	7.18	50.34	17.98	24.50
Fe-N-GC-800	6.68	0.19	0.30	6.05	38.92	36.44	18.59
Fe-N-GC-900	4.95	0.23	0.37	3.60	37.95	43.91	14.54
Fe-N-GC-1000	2.81	0.13	0.18	2.89	27.37	51.13	18.6

Table S3 The data of catalytic activity for Fe-N-GC in 0.1 M KOH electrolyte

Samples	Onset-potentail V(vs RHE)	Half-wave potential	Peak potential	J^b (mA/cm^2)
Fe-N-GC-700-p-aminotoluene	0.93	0.78	0.82	1.9
Fe-N-GC-700-p-nitroaniline	0.93	0.80	0.82	2.7
Fe-N-GC-700-2-amino pyridine	0.93	0.82	0.83	3.5
Fe-N-GC-600 (2:1)	0.91	0.71	0.79	1.0
Fe-N-GC-700 (2:1)	0.97	0.84	0.86	4.1
Fe-N-GC-800 (2:1)	0.99	0.85	0.86	4.2
Fe-N-GC-900 (2:1)	1.01	0.86	0.87	4.3
Fe-N-GC-900 (3:1)	0.97	0.85	0.85	4.5
Fe-N-GC-900 (1:1)	0.94	0.84	0.86	3.8
Fe-N-GC-1000 (2:1)	0.95	0.83	0.85	3.4
Pt/C-JM (20 μg cm^{-2})	0.99	0.83	0.85	3.3

[a] The ORR peak petential of Fe-N-GC materials obtained for their corresponding CVs

[b] The diffusion (J) limiting current density at 0.8V determined at the polarization curve at1600rmp in 0.1M KOH soultion

Table S4 The data of catalytic activity for Fe-N-GC in 0.1 M $HClO_4$ electrolyte

Samples	Onset-potentail V(vs RHE)	Half-wave potential	Peak potential	J^b (mA/cm^2)
Fe-N-GC-700-p-aminotoluene	0.77	0.54	0.60	1.9
Fe-N-GC-700-p-nitroaniline	0.79	0.63	0.63	3.7
Fe-N-GC-700-2-amino pyridine	0.82	0.54	0.69	4.8
Fe-N-GC-600 (2:1)	0.75	0.48	0.56	1.2
Fe-N-GC-700 (2:1)	0.86	0.73	0.71	5.2
Fe-N-GC-800 (2:1)	0.86	0.73	0.71	5.0
Fe-N-GC-900 (2:1)	0.88	0.74	0.71	5.3
Fe-N-GC-900 (3:1)	0.86	0.73	0.70	5.3
Fe-N-GC-900 (1:1)	0.83	0.71	0.71	4.4
Fe-N-GC-1000 (2:1)	0.83	0.70	0.69	5.0
Pt/C-JM (20 μg cm^{-2})	0.91	0.78	0.81	4.6

[a] The ORR peak petential of Fe-N-GC materials obtained for their corresponding CVs

[b] The diffusion (J) limiting current density at 0.6V determined at the polarization curve at1600 rmp in 0.1M $HClO_4$ solution